DOI: 10.1002/ejic.201100789

$[Zn(C_3H_3N_2)(C_3H_2N_2–N=N–C_6H_5)]$, a Mixed-Linker ZIF Containing a Photoswitchable Phenylazo Group

Stephan Bernt,[a] Mark Feyand,[a] Antje Modrow,[a] Julia Wack,[b] Jürgen Senker,[b] and Norbert Stock*[a]

Keywords: Metal-organic frameworks / Microporous materials / Structure elucidation / Optical switching / High-throughput methods

We report the synthesis and characterization of the new switchable Zn-based zeolitic imidazolate framework (ZIF) [Zn(Im)(aIm)] (**1**). The high-throughput investigation of the mixed linker system Zn^{2+}/imidazole (HIm)/2-phenylazoimidazole (HaIm)/DMF at 85 °C led to **1**, which is isostructural to ZIF-8 and crystallizes in a sodalite (SOD)-type structure. The preparation was also studied with microwave-assisted heating and ultrasound-assisted synthesis. The crystal structure was determined from single-crystal X-ray diffraction data. Although Im^- and aIm^- ions are present in a 1:1 molar ratio, no ordering of the 2-phenylazo group was observed. Incorporation of the Im^- and aIm^- linkers as an integral part of the framework structure was confirmed by elemental analysis, ^{13}C and ^{15}N MAS NMR, IR and Raman spectroscopy. In addition, the permanent porosity of **1** was demonstrated by N_2 sorption experiments and a specific surface area of S_{BET} = 580 $m^2 g^{-1}$ is observed. The photoswitching properties were investigated by UV/Vis spectroscopy as the *cis* and *trans* isomers exhibit different UV absorption spectra. Switching can be achieved by irradiation with UV light (λ = 355 nm), and back-switching using visible light (λ = 525 nm). Although changes in the UV/Vis spectra are detected, the switching process is only partially reversible.

Introduction

Metal-organic frameworks (MOFs) have gained increased attention in recent years due to their specific chemical and physical properties, such as pore size distribution, surface properties and chemical functionality.[1–4] They constitute a class of porous compounds that bridge the gap between microporous zeolites and ordered mesoporous silica-based materials.[5] MOFs are constructed from inorganic building units that are connected by organic linkers.[6] The choice of the linker molecule can vary the pore size, chemical functionality and physical properties such as sorption.[7,8] Functionality can be introduced directly by using functionalized linkers such as aminoterephthalic acid,[9,10] by coordination of guest molecules to unsaturated metal sites[11] or by postsynthetic covalent modification.[12,13]

Tian et al. have reported a new class of MOFs[14,15] called zeolitic imidazolate frameworks (ZIFs).[16] These compounds contain Zn^{2+} or Co^{2+} ions that are tetrahedrally surrounded by imidazolate linkers, which each bridge two Zn^{2+} or Co^{2+} ions. By employing imidazolate derivatives or mixtures thereof, various zeolitic topologies with numerous functional groups have been obtained.[17,18,19]

One goal in our current studies on MOFs is the introduction of functionality that can be modified by external stimuli. For example, sorption properties can be changed by ion exchange,[20] porosity can be switched by guest exchange[21] and the opening of pores can be triggered by gas adsorption.[22] In addition, guest-induced colour change[23] and temperature-induced cooperative spin-crossover behaviour in a 3D coordination polymer have been observed.[24] We are interested in the use of photoswitchable organic linker molecules for the synthesis of MOFs and have recently demonstrated the reversible switching of the mixed-linker MOF CAU-5, which contains azophenyl-4,4′-bipyridine and 2,6-naphthalenedicarboxylate ions.[25]

Aromatic molecules that contain azo groups, such as azobenzene or arylazoimidazole derivatives, are textbook examples for photoisomerization reactions.[26,27] In general the *trans* isomer of azobenzene is the thermodynamically more stable form[28,29] and exhibits two distinct absorption maxima. One with a lower intensity at λ_{max} = 444 nm ($n \rightarrow \pi^*$ transition) and another at λ_{max} = 316 nm ($\pi \rightarrow \pi^*$ transition). The *cis* isomer exhibits an absorption maximum at λ_{max} = 437 nm ($n \rightarrow \pi^*$ transition) and the $\pi \rightarrow \pi^*$ transition is shifted to λ_{max} = 270 nm. The *trans* isomer can be switched to the *cis* isomer by irradiation with UV light (ca. 365 nm). The switching process is schematically shown in

[a] Institut für Anorganische Chemie, Christian-Albrechts-Universität zu Kiel,
Max-Eyth-Straße 2, 24118 Kiel, Germany
Fax: +49-431-8801774
E-mail: stock@ac.uni-kiel.de
[b] Anorganische Chemie III, Universität Bayreuth,
Universitätsstr. 30, 95447 Bayreuth, Germany
Supporting information for this article is available on the WWW under http://dx.doi.org/10.1002/ejic.201100789.

Figure 1. This is clearly visible in the UV/Vis spectra as the intensity of the band at λ_{max} = 316 nm decreases and the intensity of the band at λ_{max} = 444 nm increases. Therefore, both isomers have distinct UV/Vis spectra and can easily be distinguished. The reversible back-switching can be achieved by heating or irradiation (ca. 440 nm).

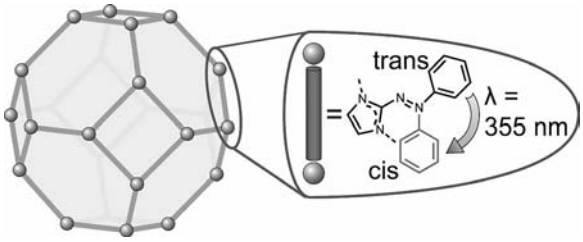

Figure 1. Schematic representation of the switching process.

MOFs containing azo groups are known in the literature.[25,30,31,32] In most of these structures the azo groups are an integral part of the linker molecules. Thus, switching is strongly hindered and has not been demonstrated to date. In contrast, reversible switching should be feasible for linker molecules with azo groups that protrude into the pores. The structure of a 1,1′-bis[(2-phenylazo)imidazol-1-yl]methane-based MOF that contains two phenylazo groups was recently published but no switching properties were shown.[33]

Here, we present the synthesis and detailed characterization of a switchable mixed-linker ZIF, [Zn(Im)(aIm)] (**1**), which contains imidazolate (Im^-) and 2-phenylazoimidazolate (aIm^-) ions.

Results and Discussion

The HaIm linker was synthesized from aniline and HIm[34] and purified by column chromatography (Figure 2). It was subsequently employed in the high-throughput investigation of the $Zn(NO_3)_2{\cdot}6H_2O$/HIm/HaIm/*N*,*N*-dimethylformamide (DMF) system. High-throughput (HT) methods allow the simultaneous investigation of different reaction parameters in solvothermal syntheses (Figure S1, Supporting Information) and are useful in the discovery of new phases and the subsequent synthesis optimization.[35] The discovery library was set up varying the solvent (DMF and methanol) and employing the molar ratios Zn^{2+}/HaIm/HIm = 1–3:1–4:0–3 (Figure 3 and Table S2). The reaction products were characterized by X-ray powder diffraction (XRPD) measurements and the results are shown in Figure 3.

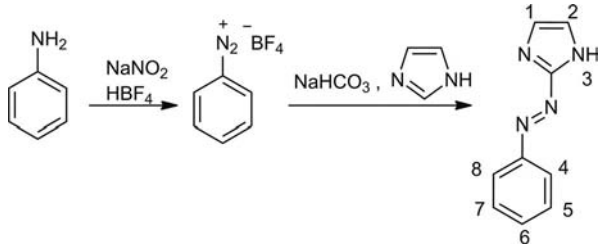

Figure 2. Synthesis of HaIm.

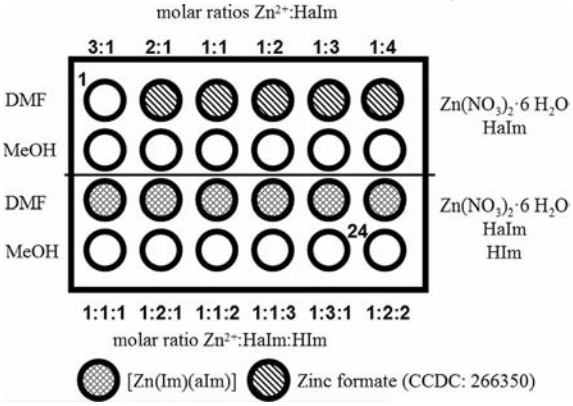

Figure 3. Discovery library of the high-throughput investigation. Empty circles denote clear solutions. The amounts used in each reactor are given in Table S2.

When HaIm was solely employed as the organic linker, reactions in methanol led exclusively to clear solutions, whereas reactions in DMF yielded zinc formate (CCDC-266350),[36] which is due to the partial hydrolysis of DMF. The mixed-linker system **1** was obtained with DMF and orange, air-stable single crystals (Figure S3) suitable for crystal structure determination were isolated from the mixture containing $Zn(NO_3)_2{\cdot}6H_2O$/HIm/HaIm/DMF in the molar ratio 1:3:1:97.

Compound **1** was also obtained using conventional heating (CH), microwave-assisted (MW) heating or ultrasound (US). The last two methods led to a substantially reduced reaction time (5 min). The three different synthetic methods resulted in phase-pure products. The CH synthesis led to large single crystals, whereas MW and US reactions yielded microcrystalline powders.

The orange, air stable compound was activated at 200 °C in vacuo for characterization by XRPD, thermogravimetric analysis (TGA), elemental analysis and IR, Raman, UV/Vis and solid-state NMR spectroscopy.

Compound **1** is isostructural to ZIF-8, which crystallizes in a sodalite (SOD)-type framework. The SOD structure has been observed in compounds that contain Zn^{2+} or Co^{2+} with 2-methyl-, 2-nitroimidazole, imidazole-2-carbaldehyde or benzimidazole (ZIF-7, -8, -9, -65, -67, -90, -91, -92).[19,37,38] Two linkers are incorporated in **1**: Im^- and aIm^-. Based on the single crystal data, no ordering of the phenylazo groups takes place. **1** is isostructural to ZIF-8 and crystallizes in the space group *I*23. Thus, we were able to establish the SOD framework as well as the position of the azo group during structure refinement (see experimental section for crystallographic data, Figures 4 and S4).

Indexing the XRPD pattern (Figures 5 and S5) unequivocally demonstrated the presence of only one crystalline phase. The lattice parameter [a = 17.009(6) Å] compares well with results from the single-crystal X-ray diffraction experiment [a = 17.023(2) Å].

The composition of activated **1** was established by elemental analysis and TGA. The observed and calculated C, H and N values compare well, and the TGA curve shows a

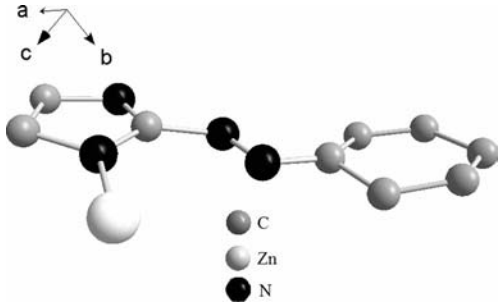

Figure 4. Asymmetric unit of **1**.

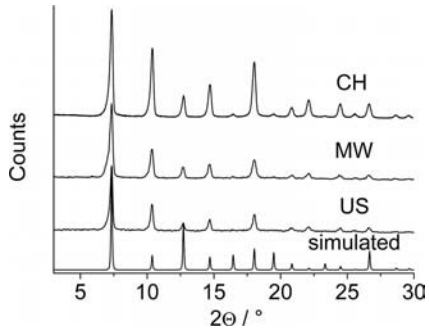

Figure 5. XRPD patterns of **1** compared to the simulated pattern, which is based on single crystal data.

weight loss of 73.14% for the CH and MW products and 66% for the US product between 340 and 700 °C (calcd. 73.54%) with ZnO as the final decomposition product (Figure S6). The incorporation of the aIm linker as part of the framework was confirmed by solid-state NMR and Raman spectroscopy (Figures 6, 7 and 8). The characteristic –N=N– asymmetric vibration band is located at 1441 cm^{-1} in the Raman spectrum, and characteristic aromatic =C–H stretching vibrations are observed between 3142 and 3047 cm^{-1}.

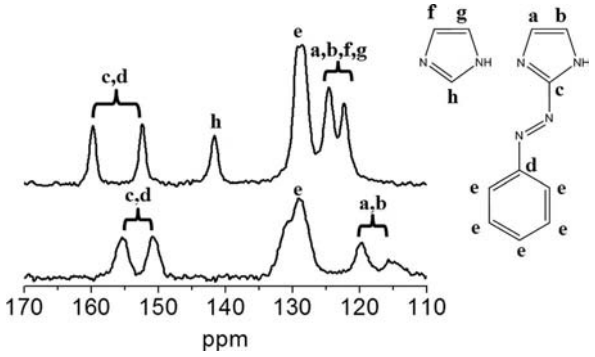

Figure 6. ^{13}C MAS NMR spectrum of **1** (top) and ^{13}C CP MAS NMR spectrum of pure HaIm (bottom).

The ^{13}C cross polarization (CP) magic angle spinning (MAS) NMR spectrum of the HaIm linker (Figure 6, bottom) shows five signals that can be clearly assigned. The signals of **1** can be assigned to both imidazolate linkers (Figures 6, top, and S8). Due to the deprotonation of HaIm and HIm, only two signals for a, b, f and g are observed,

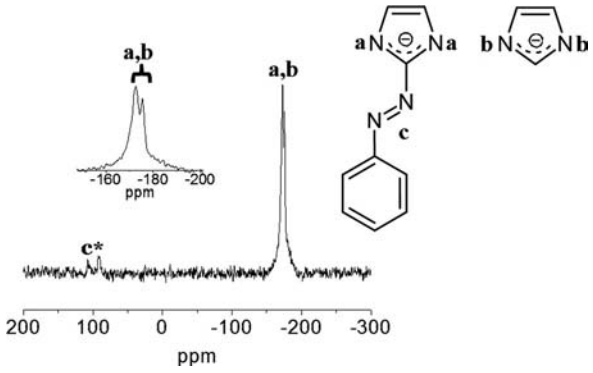

Figure 7. ^{15}N CP MAS NMR spectrum of **1**. The spinning sideband is marked with an asterisk.

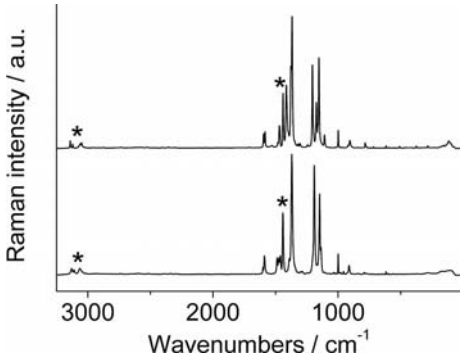

Figure 8. Raman spectra of **1** (bottom) and HaIm (top). The *trans* –N=N– vibration of **1** (1441 cm^{-1}) and the aromatic =C–H stretching vibrations (3142–3047 cm^{-1}) of the phenyl ring and the imidazolate ions are marked with asterisks.

which are shifted downfield. Two new signals (h and f, g) for Im^- are present.

The ^{15}N CP MAS NMR spectrum shows three signals that can be assigned to aIm and Im. The signal at 107 ppm is due to the nitrogen atoms of the azo group, and those at –172 and –175 ppm can be assigned to the nitrogen atoms of the imidazolate ions (Figure 7). A ^{15}N MAS NMR spectrum of the pure HaIm molecule cannot be recorded due to its very slow spin relaxation.

Although the aIm linker protrudes into the SOD cages, permanent porosity was demonstrated by N_2 sorption experiments at 77 K (Figure 9). The N_2 sorption isotherm of the activated sample (CH, 200 °C, 12 h, vacuum) shows a rapid increase at low p/p_0 values followed by a plateau, which is typical of type I isotherms. Evaluating the data with the Brunauer–Emmett–Teller (BET) equation resulted in a specific surface area (S_{BET}) of 580 $m^2 g^{-1}$ with a micropore volume (V_p) of 0.26 $cm^3 g^{-1}$. The N_2 sorption isotherms of the MW and US samples show similar behaviour but with slightly lower specific surface areas (US: S_{BET} = 544 $m^2 g^{-1}$, V_p = 0.25 $cm^3 g^{-1}$; MW: S_{BET} = 507 $m^2 g^{-1}$, V_p = 0.26 $cm^3 g^{-1}$). The specific surface area of **1** is significantly lower than ZIF-8 [S_{BET} = 1030 $m^2 g^{-1}$, V_p = 0.49 $cm^3 g^{-1}$ (calculated with PLATON as 0.54 $cm^3 g^{-1}$)], in which a methyl group protrudes into the SOD cages.[12,32]

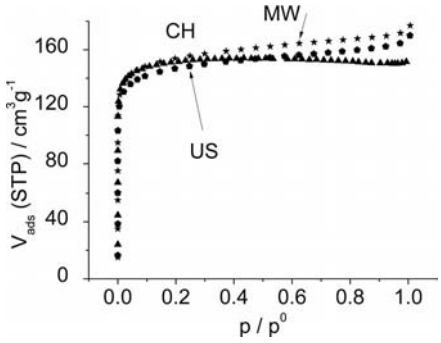

Figure 9. N_2 sorption isotherms of **1** (triangles: CH product, pentagons: US product, stars: MW product).

The switching properties of **1** were investigated using UV/Vis spectroscopy (Figures 10 and S9). Switching the azo groups from *trans* to *cis* configuration was accomplished by UV irradiation (355 nm, 150 W xenon lamp, 1 h). Back-switching was achieved by irradiation with visible light (525 nm, 150 W xenon lamp, 1 h) but not thermally (100 °C in air for 14 h). The switching of HaIm is hard to observe as fast thermal back-switching (*cis* to *trans*) takes place. In contrast, *N*-alkyl-substituted imidazolate derivatives exhibit much lower rate constants.[24,25]

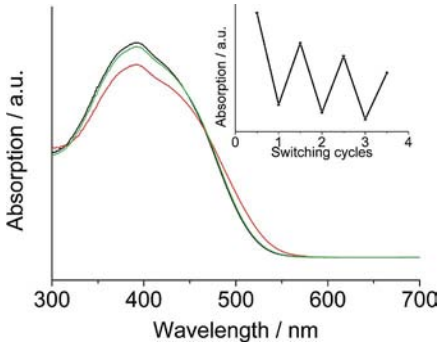

Figure 10. UV/Vis spectra of **1** before irradiation (black line), after irradiation at 355 nm for 1 h (red line) and after irradiation at 525 nm for 1 h (green line). Only one cycle is presented for clarity and more cycles are shown in Figure S9. The reversibility of the switching process (based on the π→π* absorption band at 392 nm) is shown in the inset. Every whole number represents a cycle of switching to the *cis* product and back-switching to the *trans* product.

Based on results reported for HaIm,[28,29] the bands can be assigned to the π→π* (392 nm) and *n*→π* transitions (450 nm). Upon irradiation with UV light, changes in the intensities of these bands are observed; the intensity of the π→π* band decreases, which is accompanied by an increase in the intensity of the *n*→π* band. Back-switching with visible light leads to an increase in the intensity of the π→π* band and a decrease in the intensity of the *n*→π* band. Although back-switching is not fully reversible, repeated switching and back-switching led to the corresponding changes in the UV/Vis spectra.

The partial reversibility could be due to a photobleaching effect or the steric hinderance of the switching process (confinement effect). Repeating this procedure led to the observation of the same behaviour. After three switching cycles the initial curve cannot be reached.

Conclusions

We have synthesized the porous, air-stable ZIF [Zn(Im)(aIm)] (**1**), which contains photoswitchable azophenyl groups. This compound was formed in a solvothermal reaction using a mixed-linker system. X-ray diffraction experiments demonstrated its structural relationship with ZIF-8, and the incorporation of aIm^- was proven by Raman and solid-state NMR spectroscopy. Although the large phenylazo group protrudes into the cage, **1** shows permanent prosity. UV/Vis switching experiments demonstrated the *cis–trans* isomerization and showed partial reversibility of the switching process.

Experimental Section

General: Synthetic procedures for HaIm and **1** and selected spectroscopic data are described in this section. All chemicals were used as obtained, unless stated otherwise.

2-Phenylazoimidazole (HaIm):[34] A mixture of aniline (10.6 mL, 116 mmol) and tetrafluoroboric acid (57.5 mL, 50%) was cooled to 0 °C. A solution of sodium nitrite in deionized water (18 mL) was slowly added. The precipitate was separated and washed with ethanol and diethyl ether to obtain benzenediazonium tetrafluoroborate (26.7 g).

Imidazole (6.8 g, 100 mmol) was added to a solution of sodium hydrogen carbonate (4.5 g, 53.6 mmol) in deionized water (45 mL). After homogenization of the solution, benzenediazonium tetrafluoroborate (19.2 g, 100 mmol) in deionized water (100 mL) was added. A brown precipitate formed immediately and the mixture was stirred for 30 min and allowed to stand for another 30 min. The precipitate was separated and washed with deionized water. The product was purified by column chromatography on basic aluminium oxide with ethyl acetate (+1% triethylamine) to give HaIm (9.8 g, 57%) as orange needles. $C_9H_8N_4$ (172.07): calcd. C 62.78, H 4.68, N 32.54; found C 62.54, H 4.64, N 32.61. ^{1}H NMR (200 MHz, [D$_6$]DMSO, 300 K, numbering according to Figure 2): δ = 7.38 [s, 2 H, 1,2-H], 7.6 [m, 3 H, 5,6,7-H], 7.85 [m, 2 H, 4,8-H], 13.2 [br. s, 1 H, 3-H] ppm. MS-EI: *m/z* (%) = 172.0 $[M]^+$ (77%), 144 (100), 117 (57), 105 (10); (CI) 173 $[M + H]^+$ (65%), 144 (100), 117 (48), 105 (11).

[Zn(Im)(aIm)] (1): Single crystals of **1** were formed from a solvothermal reaction in 2 mL Teflon® autoclaves in a high-throughput reactor (see Supporting Information). Solutions of $Zn(NO_3)_2{\cdot}6H_2O$ (193 μL, 0.3 M), HaIm (193 μL, 0.3 M) and imidazole (580 μL, 0.3 M) in DMF were mixed and additional DMF (433 μL) was added. The reaction mixture was heated at 85 °C in an isothermal oven for 96 h. The crystalline orange product was collected by filtration and washed with DMF (2 mL) and acetone (5 mL). The product was dried at room temperature in air for five days followed by 12 h at 200 °C in vacuo. $C_{12}H_{10}N_6Zn$ (302.03): calcd. C 47.46, H 3.32, N 27.68; found C 46.85, H 3.64, N 27.04.

Microwave-Assisted Synthesis of 1: In a typical reaction, solutions of $Zn(NO_3)_2{\cdot}6H_2O$ (193 μL, 0.3 M), HaIm (193 μL, 0.3 M) and imidazole (580 μL, 0.3 M) in DMF with additional DMF (433 μL)

were mixed in a 2 mL glass vial sealed with a Teflon®-coated cap. The reaction mixture was stirred and exposed to microwave irradiation for 5 min at 100 °C (Biotage Initiator Eight EXP). The orange solid was collected by centrifugation and redispersed in DMF (2 mL). The redispersing and centrifugation steps were repeated twice more with acetone. The product was dried at room temperature in air for five days followed by 12 h at 200 °C in vacuo. $C_{12}H_{10}N_6Zn$ (302.03): calcd. C 47.46, H 3.32, N 27.68; found C 46.86, H 3.32, N 27.42.

Ultrasound-Assisted Synthesis of 1: In a typical reaction, solutions of $Zn(NO_3)_2{\cdot}6H_2O$ (193 μL, 0.3 M), HaIm (193 μL, 0.3 M) and imidazole (580 μL, 0.3 M) in DMF with additional DMF (433 μL) were mixed in a 2 mL glass vial. The reaction mixture was sonicated using an ultrasonic generator with sonotrode (UP200S, Hielscher-Ultrasound Technology, 200 W, 24 kHz) for 10 min. The orange solid was collected by centrifugation and redispersed in DMF (2 mL). The redispersing and centrifugation steps were repeated twice more with acetone. The product was dried at room temperature in air for five days followed by 12 h at 200 °C in vacuo. $C_{12}H_{10}N_6Zn$ (302.03): calcd. C 47.46, H 3.32, N 27.68; found C 46.94, H 3.46, N 26.63.

Single-Crystal Structure Analysis: The crystal structure determination was performed with an imaging plate diffraction system (IPDS-1) with Mo-K_α radiation from STOE & CIE. The structure solution was carried out with direct methods using SHELXS-97 and structure refinements were performed against $|F|2$ using SHELXL-97. The structure solution in the space group $I\bar{4}3m$ (as found for ZIF-8) did not lead to a reasonable structure model. Choosing the subgroup $I23$ allowed the azophenyl rings to be assigned by a split model. The azophenyl rings were isotropically refined and the Zn and imidazolate ions were refined anisotropically. A numerical absorption correction was applied using X-Red (version 1.31) and X-Shape (version 2.11) of the program package X-Area. All non-hydrogen atoms were refined with anisotropic displacement parameters. Refinement of the structure led to a Flack parameter of 0.50(1). The model was therefore refined as a racemic twin using the TWIN and BASF command implemented in ShelXL. All aromatic C–H hydrogen atoms were positioned with idealized geometries and were refined with fixed isotropic displacement parameters [$U_{eq}(H) = -1.2{\cdot}U_{eq}(C)$] using a riding model with d_{C-H} = 0.93 Å. Details of the structure determination are given in Table 1.

Table 1. Selected crystal data and details of the structure determination of **1**.

Formula	$Zn_2C_{16}H_5N_{10}$
M [g mol^{-1}]	468.08
Crystal system	cubic
Space group	$I23$
a [Å]	17.023(2)
V [Å^3]	4933(1)
T [K]	293
Z	6
$D_{calcd.}$ [g cm^3]	0.945
μ [mm^{-1}]	1.472
Θ_{max} [°]	25.3
Measured reflections	19788
Unique reflections	1496
Reflections [$I_0 > 4\sigma(I_0)$]	1320
R_{int}	0.100
R_1 [all data]	0.1192
R_1 [$I_0 > 4\sigma(I_0)$]	0.1109
wR_2 [all data]	0.2717
wR_2 [$I_0 > 4\sigma(I_0)$]	0.2706
Gof	1.25
$\Delta\rho_{max}$, $\Delta\rho_{min}$ [e Å^{-3}]	0.51, –0.41

CCDC-836865 contains the supplementary crystallographic data for this paper. These data can be obtained free of charge from the Cambridge Crystallographic Data Centre via http://www.ccdc.cam.ac.uk/.

X-ray Powder Diffraction (XRPD): XRPD experiments were performed using an X′Pert Pro PANalytical Reflection Powder Diffraction System, with Cu-K_α radiation (λ = 154.0598 pm), equipped with a PIXcel semiconductor detector from PANalytical. Products of the HT investigations were characterized using a STOE HT X-ray powder diffractometer (Cu-K_α radiation) equipped with an image plate detector.

Supporting Information (see footnote on the first page of this article): Crystallographic data, HT methodology, the experimental data for the HT system where **1** was found and spectroscopic data.

Acknowledgments

We acknowledge funding from the Deutsche Forschungsgemeinschaft (DFG) (SFB 667, *Function by Switching*). We also thank Ursula Cornelissen for undertaking the Raman and UV/Vis measurements, Inke Jeß for the single crystal measurements, Adam Wutkowksi and Jan Boeckmann for the DTA/TG measurements and Dr. Frank Sönnichsen for recording solution ^{1}H NMR spectra.

[1] P. Horcajada, C. Serre, M. Vallet-Regí, M. Sebban, F. Taulelle, G. Férey, *Angew. Chem. Int. Ed.* **2006**, *45*, 5974–5978.
[2] M. Latroche, S. Surblé, C. Serre, C. Mellot-Daznieks, P. Llewellyn, J. Lee, J. Chang, S. Jhung, G. Férey, *Angew. Chem.* **2006**, *118*, 8407; *Angew. Chem. Int. Ed.* **2006**, *45*, 8227–8231.
[3] Z. Gu, X. Yan, *Angew. Chem.* **2010**, *122*, 1519–1522; *Angew. Chem. Int. Ed.* **2011**, *49*, 1477–1480.
[4] K. Tanabe, S. Cohen, *Angew. Chem.* **2009**, *121*, 7560; *Angew. Chem. Int. Ed.* **2009**, *48*, 7424–7427.
[5] G. Férey, *Chem. Soc. Rev.* **2008**, *37*, 191–214.
[6] S. James, *Chem. Soc. Rev.* **2003**, *32*, 276–288.
[7] Z. Wang, K. Tanabe, S. Cohen, *Chem. Eur. J.* **2010**, *16*, 212–217.
[8] A. Sonnauer, F. Hoffmann, M. Fröba, K. Kienle, V. Duppel, M. Thommes, C. Serre, G. Férey, N. Stock, *Angew. Chem.* **2009**, *121*, 3849; *Angew. Chem. Int. Ed.* **2009**, *48*, 3791–3794.
[9] S. Bauer, C. Serre, T. Devic, P. Horcajada, J. Marrot, G. Férey, N. Stock, *Inorg. Chem.* **2008**, *47*, 7568–7576.
[10] T. Ahnfeldt, D. Gunzelmann, T. Loiseau, D. Hirsemann, J. Senker, G. Férey, N. Stock, *Inorg. Chem.* **2009**, *48*, 3057.
[11] D.-Y. Hong, Y. K. Hwang, C. Serre, G. Férey, J.-S. Chang, *Adv. Funct. Mater.* **2009**, *19*, 1537–1552.
[12] K. K. Tanabe, S. M. Cohen, *Chem. Soc. Rev.* **2011**, *40*, 498–519.
[13] S. Bernt, V. Guillerm, C. Serre, N. Stock, *Chem. Commun.* **2011**, *47*, 2838–2840.
[14] Y.-Q. Tian, C.-X. Cai, Y. Ji, X.-Z. You, S.-M. Peng, G.-H. Lee, *Angew. Chem.* **2002**, *114*, 1442; *Angew. Chem. Int. Ed.* **2002**, *41*, 1384–1386.
[15] X.-C. Huang, Y.-Y. Lin, J.-P. Zhang, X.-M. Chen, *Angew. Chem.* **2006**, *118*, 1587; *Angew. Chem. Int. Ed.* **2006**, *45*, 1557–1559.
[16] A. Phan, C. Doonan, F. Uribe-Romo, C. Knobler, M. O'Keeffe, O. Yaghi, *Acc. Chem. Res.* **2010**, *43*, 58–67.
[17] R. Banerjee, A. Phan, B. Wang, C. Knobler, H. Furukawa, M. O'Keeffe, O. Yaghi, *Science* **2008**, *319*, 939–943.
[18] B. Wang, A. Côté, H. Furukawa, M. O'Keeffe, O. Yaghi, *Nature* **2008**, *453*, 207–211.

[19] W. Morris, C. Doonan, H. Furukawa, R. Banerjee, O. Yaghi, *J. Am. Chem. Soc.* **2008**, *130*, 12626–12627.
[20] S. Yang, X. Lin, A. J. Blake, G. Walker, P. Hubberstey, N. Champness, M. Schröder, *Nature Chem.* **2009**, *1*, 487–493.
[21] T. Maji, G. Mostafa, R. Matsuda, S. Kitagawa, *J. Am. Chem. Soc.* **2005**, *127*, 17152–17153.
[22] D. Tanaka, K. Nakagawa, M. Higuchi, S. Horike, Y. Kubota, T. Kobayashi, M. Takata, S. Kitagawa, *Angew. Chem.* **2008**, *120*, 3978; *Angew. Chem. Int. Ed.* **2008**, *47*, 3914–3918.
[23] S. Shimomura, R. Matsuda, T. Tsujino, T. Kawamura, S. Kitagawa, *J. Am. Chem. Soc.* **2006**, *128*, 16416–16417.
[24] V. Niel, J. Martinez-Agudo, M. Muñoz, A. Gaspar, J. Real, *Inorg. Chem.* **2001**, *40*, 3838–3839.
[25] A. Modrow, D. Zargarani, R. Herges, N. Stock, *Dalton Trans.* **2011**, *40*, 4217–4222.
[26] J. Griffiths, *Chem. Soc. Rev.* **1972**, *1*, 481–493.
[27] H. Dürr, H. Bouas-Laurent, in: *Photochromism*, Elsevier, Amsterdam **1990**, vol 1.
[28] J. Otsuki, K. Suwa, K. Narutaki, C. Sinha, I. Yoshikawa, K. Araki, *J. Phys. Chem. A* **2005**, *109*, 8064–8069.
[29] J. Otsuki, K. Suwa, K. Sarker, C. Sinha, *J. Phys. Chem. A* **2007**, *111*, 1403–1409.
[30] T. Reineke, M. Eddaoudi, D. Moler, M. O'Keeffe, O. Yaghi, *J. Am. Chem. Soc.* **2000**, *122*, 4843–4844.
[31] Z.-F. Chen, R.-G. Xiong, B. Abrahams, X.-Z. You, C.-M. Che, *J. Chem. Soc., Dalton Trans.* **2001**, *17*, 2453–2455.
[32] V. Zeleňák, Z. Vargová, M. Almáši, A. Zeleňáková, J. Kuchár, *Microporous Mesoporous Mater.* **2010**, *129*, 354–359.
[33] C.-M. Jun, Z. Zhu, Z.-F. Chen, Y.-J. Hu, X.-G. Meng, *Cryst. Growth Des.* **2010**, *10*, 2054–2056.
[34] R. Verma, M. Aggarwal, M. Bansal, I. Kaur, *Med. Chem. Res.* **2007**, *15*, 483–491.
[35] N. Stock, *Microporous Mesoporous Mater.* **2010**, *129*, 287–295.
[36] H. F. Clausen, R. D. Poulsen, A. D. Bond, M.-A. S. Chevallier, B. Brummerstedt Iversen, *J. Solid State Chem.* **2005**, *178*, 3343–3351.
[37] K. Park, Z. Ni, A. Côté, J. Choi, R. Huang, F. Uribe-Romo, H. Chae, M. O'Keeffe, O. Yaghi, *Proc. Natl. Acad. Sci. USA* **2006**, *103*, 10186–10191.
[38] A. Phan, C. Doonan, F. Uribe-Romo, C. Knobler, M. O'Keeffe, O. Yaghi, *Acc. Chem. Res.* **2010**, *43*, 58–67.

Received: July 28, 2011
Published Online: October 26, 2011

